

周丽平, 孙怡, 程凯, 等. 工业 X 射线 CT 中基于深度学习的射束硬化伪影抑制方法 (英) [J]. CT 理论与应用研究, 2018, 27(2): 227-240. doi:10.15953/j.1004-4140.2018.27.02.11.
Zhou LP, Sun Y, Cheng K, et al. Deep learning based beam hardening artifact reduction in industrial X-ray CT[J]. CT Theory and Applications, 2018, 27(2): 227-240. doi:10.15953/j.1004-4140.2018.27.02.11.

Deep Learning Based Beam Hardening Artifact Reduction in Industrial X-ray CT

ZHOU Li-ping, SUN Yi[✉], CHENG Kai, YU Jian-qiao

School of Information and Communication Engineering,
Dalian University of Technology, Dalian 116024, China

Abstract: In the nondestructive detection with industrial CT, due to the fact that the actual X-ray source has a wide spectrum, slices reconstructed by most existing reconstruction algorithms will suffer from beam hardening artifacts. It will degrade image quality greatly, affecting important CT image task such as CT diagnosis and so on. In this study, we propose a method to suppress beam hardening artifacts based on deep learning. We train a convolutional neural network using a large number of images with beam hardening artifacts as input and the corresponding artifact-free images reconstructed at a fixed energy as output to establish the mapping between image with beam hardening artifacts and artifact-free image for suppressing beam hardening artifacts. Experimental results show the effectiveness of the proposed method in the beam hardening artifact reduction of CT images.

Keywords: beam hardening; CT; deep learning; convolutional neural network

doi:10.15953/j.1004-4140.2018.27.02.11

CLC number: O 242

Document code: A

X-ray CT has been widely used in medical diagnosis and industrial nondestructive detection field^[1]. Due to the wide energy spectrum of actual X-ray source, the low-energy photons are easier to be absorbed than high-energy photons so the average energy of the photons after passing through the object become higher. As a result, the CT images directly reconstructed by the most existing algorithms which are based on the assumption that the X-ray source is monochromatic will show image artifacts. These artifacts are called beam hardening artifacts. Beam hardening artifacts seriously affect CT diagnosis or industrial detection results.

Beam hardening artifacts have been a research hotspot for decades and many artifact reduction strategies are developed. These methods can roughly be divided into four categories: physical filtration, linearization, dual-energy systems and statistical polychromatic reconstruction.

Physical filtration method reduces the artifacts by adding a filter between the X-ray source and detector to absorb the low-energy photons of the beam^[2]. However, since some photons are absorbed, the signal to noise ratio also decreases. If the filter is not thick enough, beam hardening artifacts still remain.

Linearization method reduces beam hardening artifacts by transforming the measured polychromatic attenuation data into monochromatic attenuation data^[3-5]. Usually the phantom composed of the same material as the specimen is required to calibrate the mapping from polyenergetic data to monoenergetic data. Some Linearization method may estimate the mapping

Date of Receiving: 2017-08-12.

Foundation item: National Key scientific Instrument and Equipment Development Projects (2014YQ240445).

from the reconstructed slices directly, but segmentation procedure is required. The quality of corrected slices is very sensitive to the segmentation accuracy, and moreover, the correction model should be calculated again once the scanning spectrum has been changed.

In dual-energy methods^[6-8], the attenuation coefficient is modeled as a linear combination of two basic functions. The most commonly used basis function is the function related to the photoelectric and the Compton Scatter. Projection data at different energies are required. However, this lead to the need of two X-ray sources and detectors or two scans.

Statistical polychromatic reconstruction method reduces beam hardening artifacts by accounting for the polychromatic nature of X-ray source^[9]. The method requires two steps: first the physical phenomena of data formation is modeled, then the image is reconstructed by a statistical iterative technique. Chen et al^[10] proposed to separate the polychromatic energy spectrum into several sub-energy spectrum and then make parameter estimation with the statistical method on the basis of traditional reconstruction algorithm to remove the cupping artifact. Van Gompel et al^[11] got several materials by segmentation based on density and divide the energy spectrum into several bins. The attenuation coefficient of materials at every energy bin can be obtained by minimizing the differences between the polychromatic projection and the simulated projection. Elbakri et al^[12] proposed a method with no segmentation process. They first modeled the attenuation coefficient of each pixel as the product of its unknown density and a weighted sum of energy-dependent mass attenuation coefficients. A penalized-likelihood function was formulated and the unknown density of pixel was calculated by iterative procedure. The statistical polychromatic reconstruction methods are often time-consuming, which limits its application in practice.

Besides above methods, there are some other beam hardening artifact reduction methods. Brabant et al^[14] proposed an artifact correction method based on the simultaneous algebraic reconstruction technique (SART) in which the polychromatic project process was included. Park et al^[15] derived an expression of difference between the original uncorrected image and the ideal corrected image related to the objects of high density. And the method removed beam hardening artifacts without the use of sinogram data. However, intensive computation was often required.

The existing methods to reduce beam hardening artifacts have achieved good performance in some cases. But most of the aforementioned methods have some problems in practical application. It is necessary to search a new method to reduce beam hardening artifacts. Recently, Deep learning, which can learn many features from images using multilayer network has achieved a great success in the field of computer vision such as image semantic segmentation, image de-noising, super-resolution and so on^[16-18]. In medical imaging, the great achievements based on convolutional neural network in CT image segmentation^[19], organ classification^[20], image reconstruction^[21], low-dose CT image de-noising^[22], and limited angle CT image artifacts suppressing^[23] have shown that deep learning is an effective way to solve some traditional CT problems.

Recently, Park et al^[24-25] have shown that beam hardening artifacts have some characteristics. Streaking artifacts occur along the lines tangent to the boundary of two metallic objects. At the same time, cupping artifacts are characterized that in a homogeneous object, the CT value of inner region is lower than the outer. So the beam hardening artifacts show some common characteristics. Since convolutional neural network can adaptively learn features from images, which is suitable for beam hardening artifact reduction.

Inspired by the amazing achievements of deep learning in image processing and the fact that beam hardening artifacts have some characteristics, we propose a method to reduce beam hardening artifacts with deep convolutional neural network. The inputs of the network are images reconstructed with poly-energetic data by FBP algorithm and the output are artifact-free images

reconstructed at a fixed energy. The proposed method neither needs hardware filter nor dual-energy scanning system. A large number of data are simulated to train the network, and the trained network is used to reduce beam hardening artifacts of images reconstructed by real CT system. Furthermore, compared with linearization method, the convolutional neural network trained with a large number of data can learn and predict the law of artifacts, which makes the trained network work for the artifact reduction of the same material at each spectrum.

The rest of the paper is organized as follows. In section 1 the method is given in detail. In section 2, experimental results are presented. Finally, the conclusion is given in section 3.

1 Methods

Beam hardening is a process that the average energy of X-ray increases after the beam propagates through a material since the X-ray of lower energy is preferentially absorbed. The slices which are reconstructed based on linear Radon model will show beam hardening artifacts. In this section, firstly the reason and characteristics of beam hardening artifacts are introduced. Then convolutional neural network based beam hardening artifact reduction method is presented in detail.

1.1 Beam hardening artifact

According to Beer law, the intensity of mono-energetic X-ray passing through a single material can be expressed by

$$I = I_0 \exp(-\mu x) \quad (1)$$

Where I_0 is the initial intensity and I is the intensity after the X-ray beam passes through the object, μ is attenuation coefficients of the material, x is the length traversed through the material by the X-ray. But when the X-ray is ploy-energetic, the attenuation coefficients μ is not a fixed value and varies with the energy. So Eq.(1) becomes:

$$I = \int_{E_{\min}}^{E_{\max}} I_0(E) \exp\left(-\int_L \mu(x, y, E) dl dE\right) \quad (2)$$

Where $I_0(E)$ is the initial intensity of X-ray beam at energy E . Most of the existing reconstruction algorithms presume that the X-ray source is mono-energetic and the attenuation coefficient is independent of energy. Then the slices reconstructed by these algorithms with polychromatic projection data will show artifacts, which are called beam hardening artifacts. Ideally, there is a linear relationship between the projection data and the thickness of X-ray passing through in the case of the single material object. But the relationship is not linear in practice. The thicker the X-ray passes through the object, the greater the deviation between the polychromatic projection and the ideal monochromatic projection is. The relationship between real projection (p) and the thickness (x) of

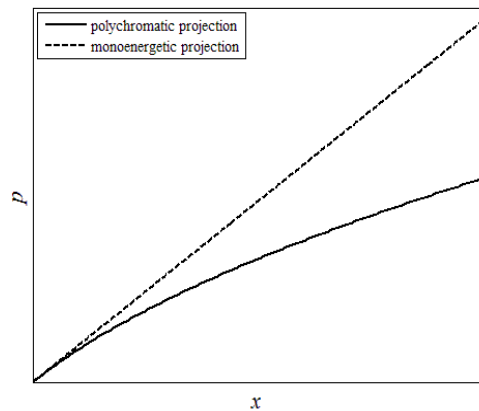


Fig.1 The relationship between real projection and the thickness of X-ray passing through the object

X-ray passing through the object is shown in Fig.1.

Beam hardening artifacts have two main manifestations in tomographic images: cupping artifacts and streaking artifacts. The display of the cupping artifacts is that the gray value of region near the edge is higher than the gray value of the center region. And the shape of the reconstructed slice of a homogeneous cylinder is similar to the bottom of a cup. Streaking artifacts display as the dark and bright streaks between objects, especially severe in the region tangent to the boundaries of two objects. The cupping artifacts and streaking artifacts are displayed in Fig.2. If the slice is composed of one cylinder at the center of the image, as shown in Fig.3(a), the polychromatic projection data at the edge of the cylinder can be approximately equal to the ideal monochromatic projection. So the gray value of the reconstructed region at the edge of the cylinder is approximately equal to the gray value reconstructed with the ideal monochromatic projection. But at the center of the cylinder there is big difference between the polychromatic and monochromatic projection. Then the gray value at the central region of the cylinder is smaller than that of the edge region. Since all the projections are back projected, cupping artifacts will appear. Fig.3 (b)-(c) shows the characteristics of cupping artifacts. The larger cylinder diameter leads to the smaller gray value.



Fig.2 Visual display of cupping and streak artifacts

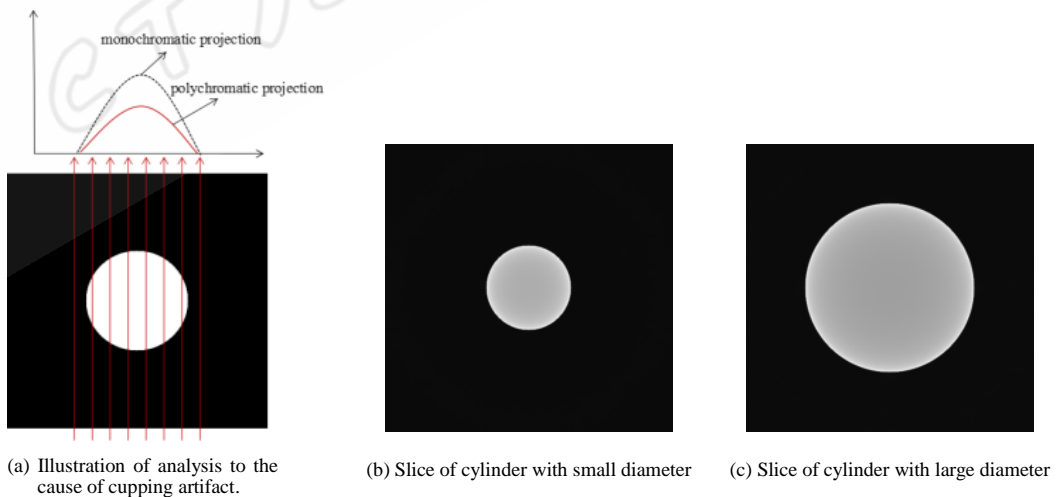


Fig.3 Illustration of analysis to the cause of cupping artifact and the characteristics of cupping artifacts

Park et al.^[24-25] have demonstrated that the shape of metal streaking artifacts are mainly caused by the metal region with polychromatic X-ray source. The beam hardening correction factor of discrepancy between polychromatic projection and the Radon transform of the image is

derived. They proved mathematically that streaking artifacts occur along the lines tangent to boundaries of two metallic objects. The reconstructed slices composed of two cylinders of different distances with streaking artifacts are shown in Fig.4.

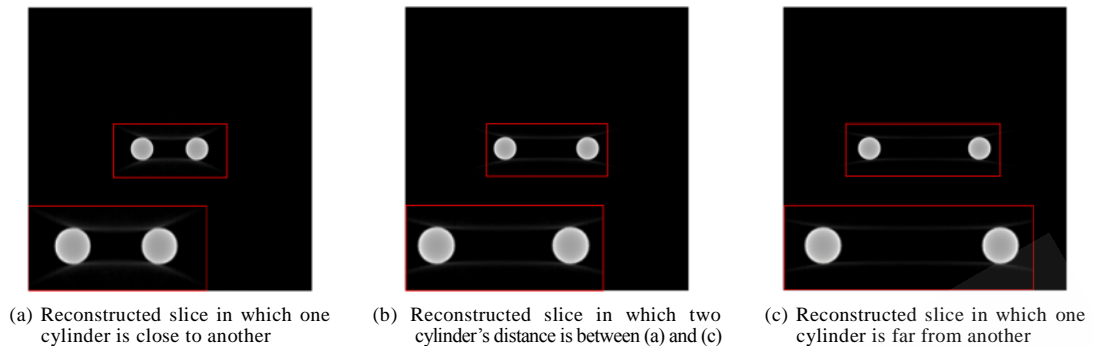


Fig.4 Reconstructed slice with different distance between two cylinders

It can be seen from the above two groups of simulation that the severity of the cupping artifacts is related to the thickness of the X-rays passing through the object. The thicker X-ray passes through the object, the smaller gray value of the reconstructed object is. The severity of the streaking artifacts is related to the distance between the two objects in the slice. The closer distance between the two cylinders results in more serious streaking artifacts.

1.2 Deep learning based beam hardening artifact reduction

The above simulations show that the cupping artifacts and streaking artifacts have certain regularity. In consideration of characteristics of beam hardening artifacts as shown in Fig.2-4, features about artifacts can be extracted from the reconstruction slices via convolution, and then reconstruction slices can be rectified by nonlinear filtering the features after mapping to a higher dimension. If the training data is enough, the convolutional neural network can learn this nonlinear filtering (non-linear mapping) to reduce beam hardening artifacts.

Although the network with more layers will show better performance, it will cost more time on training. And three layers network can learn enough features of artifacts from slices, so here we choose a convolutional neural network with three layers. These layers are all convolutional layers. Fig.5 shows the architecture of the network.

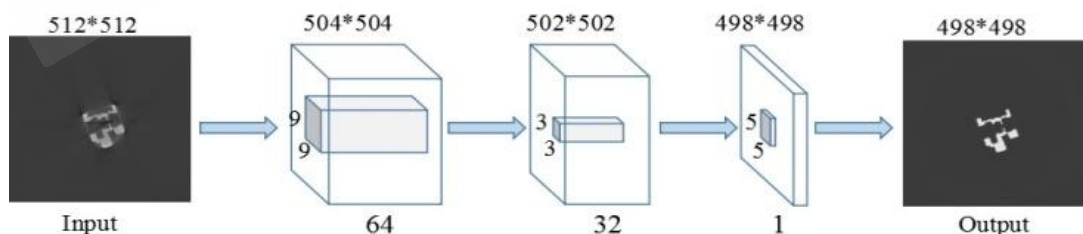


Fig.5 The architecture of convolutional neural network used in this paper.

The images with beam hardening artifacts reconstructed by FBP algorithm are the input of the network and the artifact-free images reconstructed at a fixed energy are the output. These three layers can be seen as the procedures of feature extraction, non-linear filtering, and feature combination. Process of each layer is formulated as follows:

$$\text{First layer: } f_1(x) = \text{ReLU}(W_1 * x + b_1) \quad (3)$$

$$\text{Second layer: } f_2(x) = \text{ReLU}(W_2 * x + b_2) \quad (4)$$

$$\text{Third layer: } f_3(x) = W_3 * x + b_3 \quad (5)$$

Here x denotes the input of each layer and $f_1(x)$, $f_2(x)$, $f_3(x)$ are outputs of each layer, W_1 , W_2 , W_3 denote the weights of each layer and b_1 , b_2 , b_3 are the biases respectively. The ReLU activation function is adopted in the network in order to reduce the interdependence of weights of the network and accelerates the convergence speed of training the network.

The parameters of the network for beam hardening artifact reduction of homogeneous object are described as follows. The first layer is the feature extraction layer. In this paper, 64 convolution kernels in size of 9×9 are selected to convolve with the input image and the sliding step of the convolution kernels is 1. Thus, 64 different feature maps will be obtained after the transformation of the ReLU activation function. The second convolution layer is a nonlinear mapping layer. 32 convolution kernels in size of 3×3 are convolved with the output of the first layer and 32 different feature maps are obtained after ReLU nonlinear transformation. The third layer is the feature combination layer, using a 5×5 kernel to convolve with the output of the second layer and the final output is obtained. Fig.6 shows the input image with beam hardening artifacts.



Fig.6 The input image with beam hardening artifacts

The beam hardening artifact reduction problem is solved by three steps: feature extraction, nonlinear mapping and result reconstruction.

The three steps are introduced as follows.

1.2.1 Feature extraction

The first convolution layer is to extract a series of features of the input slice including the edges, angles, contours and other information of the input slice. At the same time, features of the dark streaking, bright streaking and cupping artifacts are extracted too.

Fig.7 shows the output images after the first layer, and some output images such as (8), (16), (37), (44), (64) extract the edge, angle and contour information. Some output images such as (23) and (27) extract the dark streaking artifacts, similarly some extract the bright streaking artifacts such as (34), (58), and some complete the information extraction of cupping artifacts such as (17), (33), (60).

1.2.2 Nonlinear mapping.

The second convolution layer maps a series of features extracted from the first layer to a higher dimension, and the operation of this layer has a stronger effect on the beam hardening artifact reduction. In this layer, the artifacts and the objects are almost separated. The output of the second layer is shown in Fig.8, where some output images show the information about artifacts such as (12), (26), (30), other images such as (24) rarely contain the information of beam hardening artifacts.

1.2.3 Result reconstruction.

This layer combines the extracted image features to reconstruct the final result which does not contain beam hardening artifacts. The image after hardening artifact reduction is shown in Fig.9.

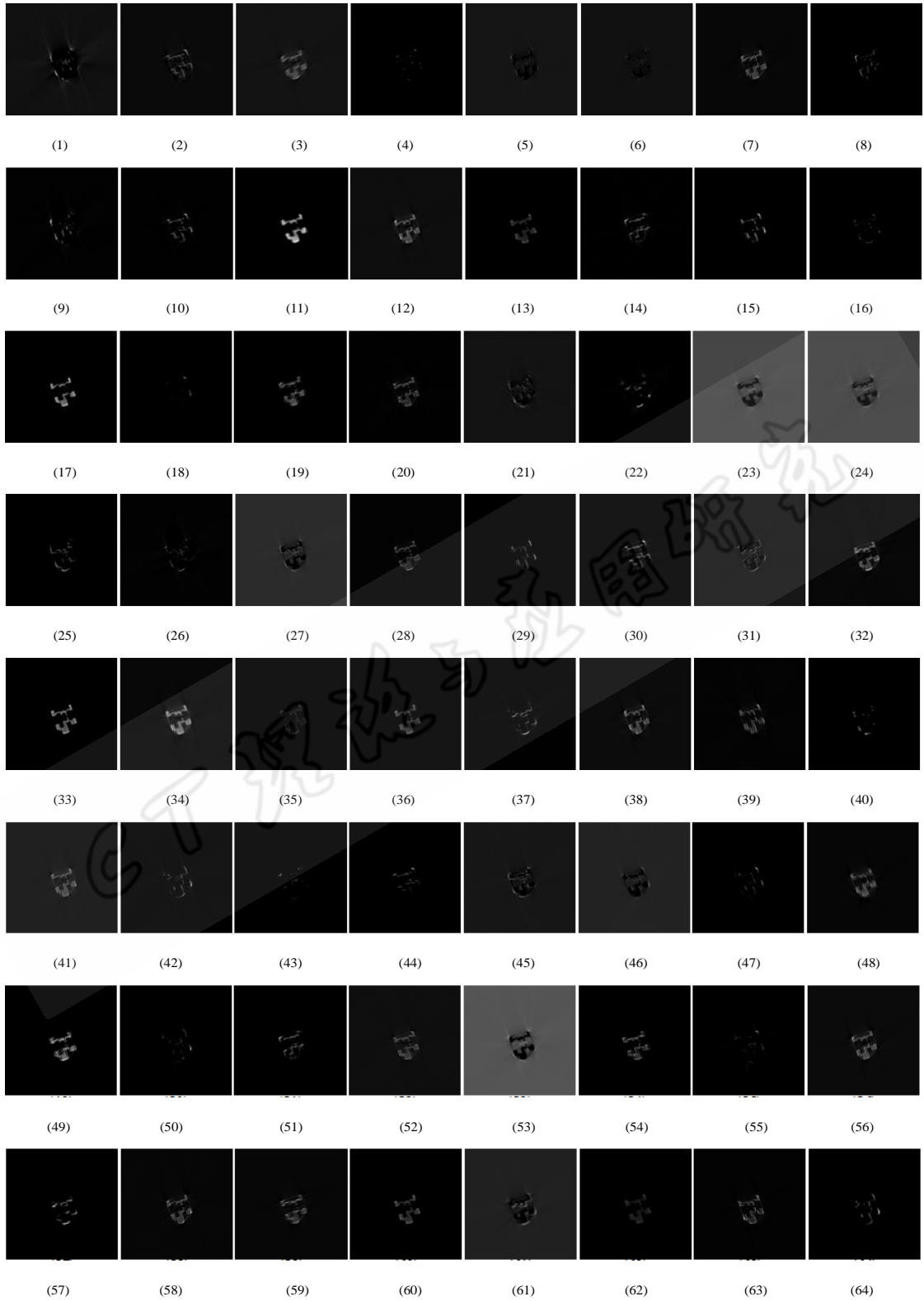


Fig.7. Results of input image after the first convolutional layer

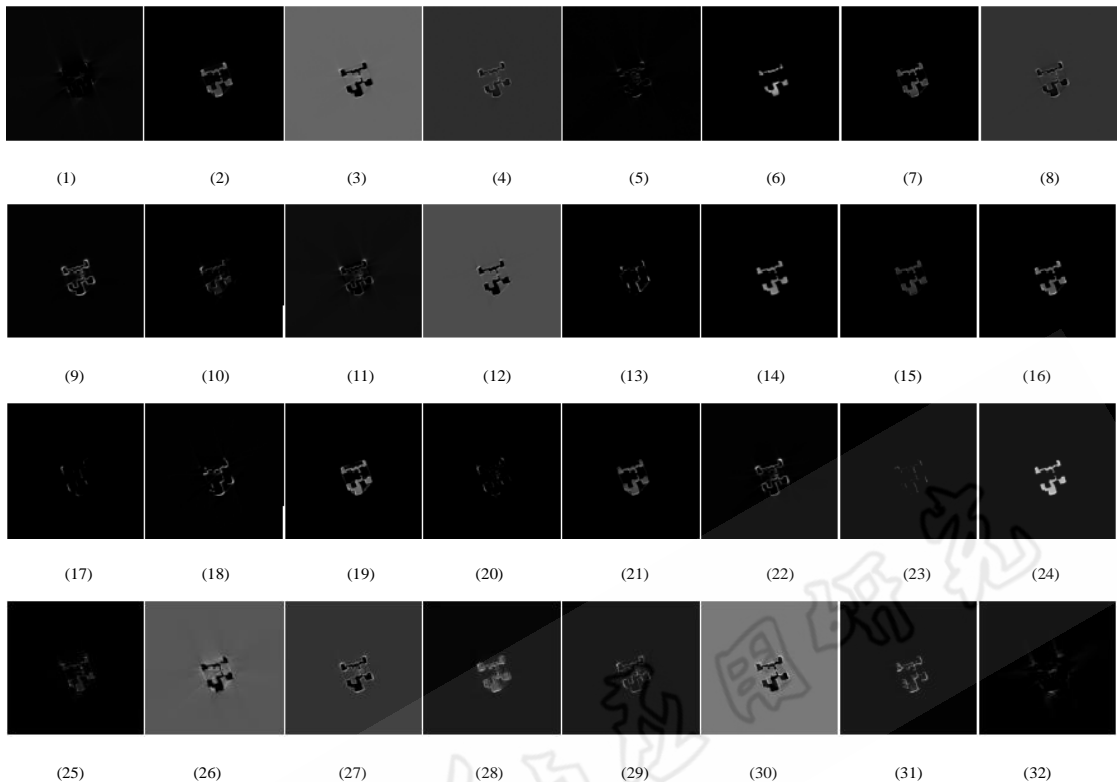


Fig.8 Some results of the second convolutional layer

2 Experiments and Results

In this section, dataset preparation is introduced in detail. Then experimental results tested with simulated data and real data are presented.

2.1 Dataset preparation

From the analysis above we can see that the size of object affects the severity of cupping artifacts and the distance of two objects also influences severity of streaking artifacts. To make the convolutional neural network learn the regularity of beam hardening artifacts, the objects in training data should include enough variations on the size, distance and locations. Due to the fact that real work pieces have limited shapes and geometry structures, it is hard to include enough variations. So in this paper we generate training data by simulation.

We generate a large number of initial images with different object size, distance between objects, and locations, which is realized by randomly selecting several basic shapes of circles, squares, ovals and rectangles with different sizes to form an image with rotation and translation transform. And we use data reconstructed with projections collected at

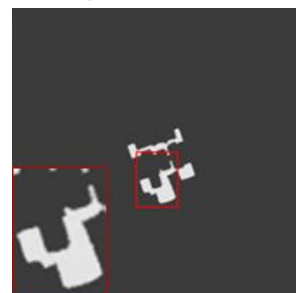


Fig.9 The final result of the network

several voltages to train the network, so the trained network can reduce artifact of images obtained at these voltages. In this paper the images are scanned at the voltage of 120 kV, 135 kV, and 150 kV respectively with the circuit of 2 mA and copper is used as the simulation material. The slices are reconstructed by FBP method. Fig.10 shows the spectrum of 120 kV, 135 kV and 150 kV where the Y -axis denotes the number of photons at each energy, and the copper's variation curve of attenuation coefficient A with energy E is shown in Fig.11.

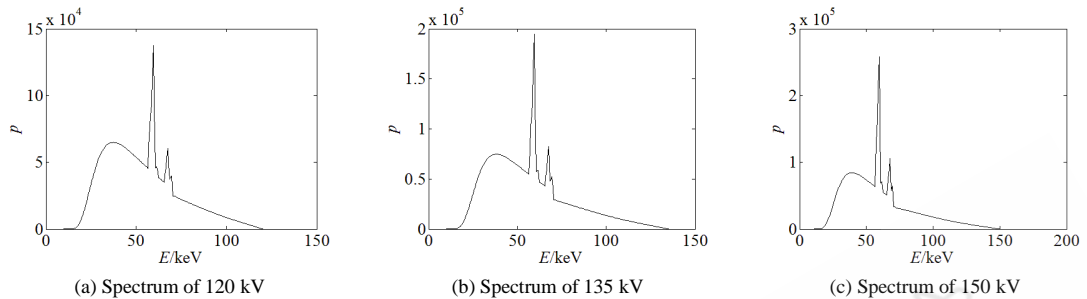


Fig.10 The energy spectra of three voltages

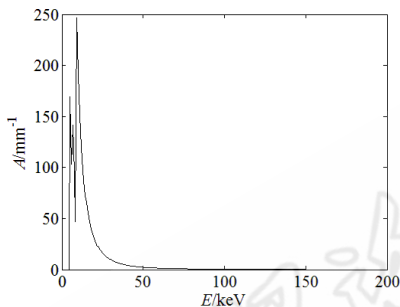


Fig.11 Variation curve of copper attenuation coefficient with energy

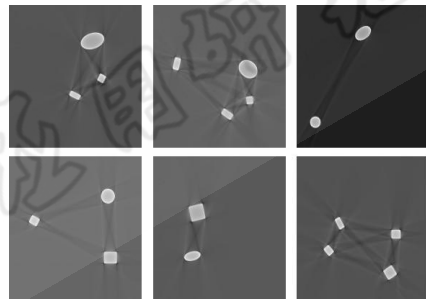


Fig.12 Some input images to train the network

In this paper, images with size of 512×512 are scanned by parallel-beam geometry. 720 projections are uniformly sampled over 180 degrees while the 1D detector contains 768 bins. The slices reconstructed from polychromatic projections by FBP algorithm will show beam hardening artifacts. The slices with artifacts are used as the input of network and those reconstructed with monochromatic projections at a fixed energy are the output. Here the fixed energy is set to 74keV. 400 images are generated at each voltage, 370 of which are the training data and the rest 30 are for testing. Hence there are 1110 images for training and 90 images for testing with three voltages in total. Some of the input images are shown in Fig.12.

2.2 Results tested with simulated data

The convolutional neural network proposed in this paper is trained under the open source framework of caffe^[26] running on a PC with NVIDIA GTX TITAN X graphics card. The initial weights of filters in each layer are randomly set, which satisfy the Gaussian distribution with zero mean and standard deviation 0.001. The loss is computed as the Euclidean distance between the artifact corrected image and ground truth (the artifact-free image). The loss function is optimized using the stochastic gradient descent method. The learning rate is 0.00001 and the training process takes roughly 18 hours.

The trained network is tested with reconstructed images scanned at voltage of 120 kV,

135 kV, 150 kV respectively. Fig.13 to Fig.15 illustrate some testing results of the trained convolutional neural network. All the uncorrected images present severe beam hardening artifacts. The artifacts of images corrected with the proposed method in this paper are largely reduced. For example, we can see the streaking artifacts clearly in Fig.15(a), whereas these artifacts are removed in Fig.15(b), thus the edges look much sharper.

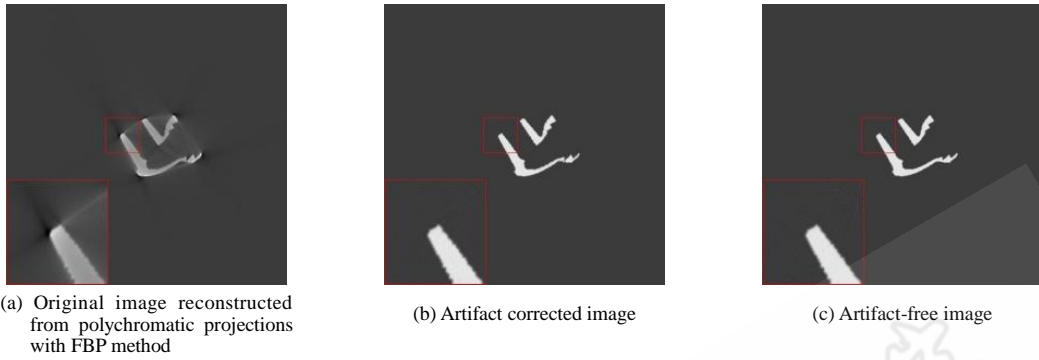


Fig.13 Testing results of 120 kV

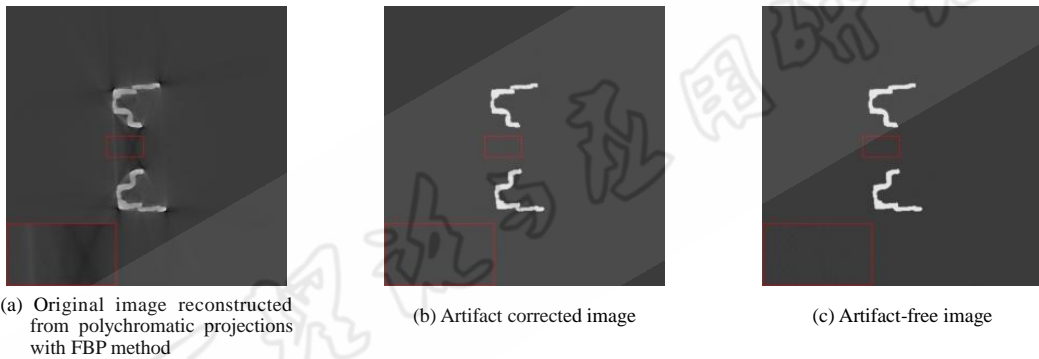


Fig.14 Testing results of 135 kV

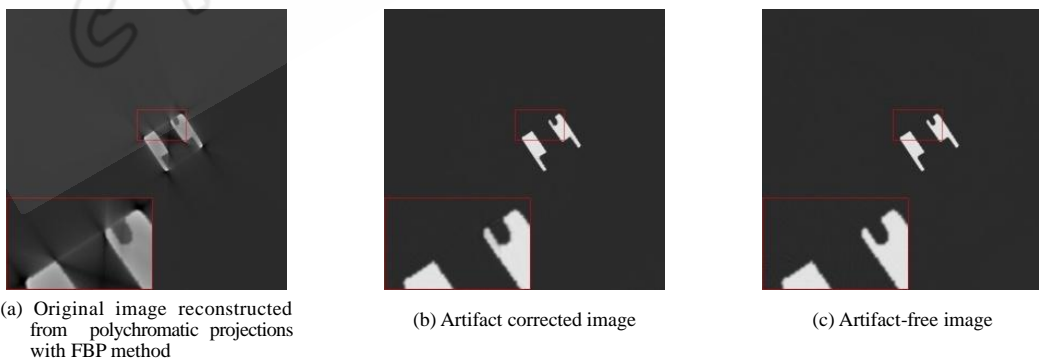


Fig.15 Testing results of 150 kV

The experimental results validate the effectiveness of the proposed method for beam hardening artifact reduction of the reconstructed slices. This is mainly because the beam hardening artifacts in images present some characteristics, and the network trained with a large number of data can learn the relationship between images with artifacts and the corresponding artifact-free images. Then beam hardening artifacts can be suppressed.

Simultaneously, the testing results demonstrate that the proposed method can reduce the artifacts of images scanned at several different voltages.

2.3 Results testing with real data

To validate the effectiveness of our method for real data, several copper cylinders are used. The reason why we select copper is that beam hardening artifacts in reconstructed slices of copper is quite severe and the correction of artifacts in copper slices is very necessary. In this paper, we correct the slices reconstructed by real CT system with the simulated trained network. In the experiment with real CT system, the work pieces to be scanned are a group of copper cylinders.



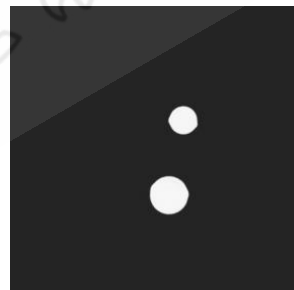
Fig.16 The copper used in the real experiment

Table 1 Parameters of scanning

Parameters	Value
Voltages	100 kV, 120kV
Distance between source and rotation axis	800.0 mm
Distance between source and detector	1 080.0 mm
Pixel size of detector	0.2 mm
Resolution of detector	1 024
Number of projections	360

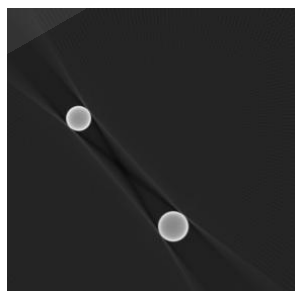


(a) Uncorrected image reconstructed by FBP method

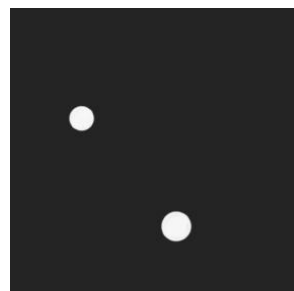


(b) Artifact corrected image with the proposed method

Fig.17 Experimental results with real data at 120 kV



(a) Uncorrected images reconstructed by FBP method



(b) Artifact corrected images with the proposed method

Fig.18 Experimental results with real data at 100 kV

The diameters of the copper cylinders are 4mm, 5mm, 6mm and 8mm respectively. The copper cylinders used in this experiment are shown in Fig.16 and resolution of reconstructed slice

is 512×512 with pixel size of $0.1105 \text{ mm} \times 0.1105 \text{ mm}$. The parameters of fan-beam scanning are shown in table 1.

The copper cylinders with diameters of 6 mm and 8mm are scanned at the voltage of 120 kV. Beam hardening artifacts of the slice are corrected by the simulated trained network. Fig.17 shows the experimental results using the proposed correction method. From Fig.17, we can see that the uncorrected image directly reconstructed by FBP displays severe artifacts including cupping artifacts and streaking artifacts. But the image corrected with the proposed method shows little cupping or streaking artifacts. The result preliminarily proves the effectiveness of the method proposed in this paper.

To study the correction effect of the proposed method for images reconstructed with projections scanned at other voltage, we correct the slices scanned at 100 kV with the trained network. Fig.18 shows the uncorrected image and the corrected image respectively. We can see the artifacts of the image scanned at 100 kV are greatly reduced. This is because the trained network can learn the regularity of beam hardening artifacts and is able to reduce the image artifacts scanned at 100 kV to some extent. If the training data contain images reconstructed at enough spectrums, the trained network can work for artifact reduction of images at different spectrums.

The experimental results in Fig.17 and Fig.18 illustrate the effectiveness of the proposed method for beam hardening artifact reduction and the method proposed in this paper can work for a relatively wide spectrum.

3 Conclusion

The beam hardening artifacts severely degrade the quality of images reconstructed by most existing methods in practical X-ray CT reconstruction. In this study a convolutional neural network is proposed to suppress the beam hardening artifacts in reconstructed images. The network can learn the regularity of artifacts and give the images with little artifacts.

The main limitation of our method is that the training process is time-consuming. This can be solved by the acceleration with high performance computing graphic cards or distributed computing systems. Besides, a large number of data should be generated to train the network.

In conclusion, this paper proposes a method to suppress beam hardening artifacts based on convolutional neural network. The inputs of the network are slices reconstructed with polychromatic projection data by FBP algorithm. The artifact-free slices reconstructed at a fixed energy are the output of the network. The experimental results demonstrate the effectiveness of the proposed method.

Reference

- [1] Wang G, Yu H, De MB. An outlook on X-ray CT research and development[J]. *Medical Physics*, 2008, 35(3): 1051-1064.
- [2] Jennings RJ. A method for comparing beam-hardening filter materials for diagnostic radiology[J]. *Medical Physics*, 1988, 15(4): 588-599.
- [3] Herman GT. Correction for beam hardening in computed tomography[J]. *Physics in Medicine and Biology*, 1979, 24(1): 81-106.
- [4] Yan CH, Whalen RT, Beaupre GS, et al. Modeling of polychromatic attenuation using computed tomography reconstructed images[J]. *Medical Physics*, 1999, 26(4): 631-642.
- [5] Hsieh J, Molthen RC, Dawson CA, et al. An iterative approach to the beam hardening correction in

- cone beam CT[J]. *Medical Physics*, 2000, 27(1): 23-29.
- [6] Marshall Jr WH, Alvarez RE, Macovski A. Initial results with prereconstruction dual-energy computed tomography (prepect)[J]. *Radiology*, 1981, 140(2): 421-430.
- [7] Ying Z, Naidu R, Crawford CR. Dual energy computed tomography for explosive detection[J]. *Journal of X-ray Science and Technology*, 2006, 14(4): 235-256.
- [8] Li B, Zhang Y. Projection decomposition algorithm of X-ray dual-energy computed tomography based on projection matching[J]. *Acta Optica Sinica*, 2010, 31(3): 0311002.
- [9] Elbakri A, Fessler JA. Statistical image reconstruction for polyenergetic X-ray computed tomography[J]. *IEEE Transactions on Medical Imaging*, 2002, 21(2): 89-99.
- [10] 陈慧娟, 潘晋孝. 一种基于多能统计的射束硬化校正方法[J]. *CT 理论与应用研究*, 2010, 19(1): 13-27.
- Chen HJ, Pan JX. A beam-hardening correction method based on poly-energetic statistics in X-ray CT[J]. *CT Theory and Applications*, 2010, 19(1): 13-27. (in Chinese).
- [11] Van Gompel G, Van Slambrouck K, Defrise M, et al. Iterative correction of beam hardening artifacts in CT[J]. *Medical Physics*, 2011, 38(1): 36-49.
- [12] Elbakri A, Fessler JA. Segmentation-free statistical image reconstruction for polyenergetic X-ray computed tomography with experimental validation[J]. *Physics in Medicine and Biology*, 2003, 48(15): 2453.
- [13] 张俊, 李磊, 张峰, 等. X 射线 CT 射束硬化校正方法综述[J]. *CT 理论与应用研究*, 2013, 22(1): 195-204.
- Zhang J, Li L, Zhang F, et al. Review of the methods for beam hardening correction in X-ray computed tomography[J]. *CT Theory and Applications*, 2013, 22(1): 195-204. (in Chinese).
- [14] Brabant L, Pauwels E, Dierick M, et al. A novel beam hardening correction method requiring no prior knowledge, incorporated in an iterative reconstruction algorithm[J]. *Nondestructive Testing and Evaluation International*, 2012, 51: 68-73.
- [15] Park HS, Hwang D, Seo JK. Metal artifact reduction for polychromatic X-ray CT based on a beam-hardening corrector[J]. *IEEE Transactions on Medical Imaging*, 2016, 35(2): 480-487.
- [16] Long J, Shelhamer E, Darrell T. Fully convolutional networks for semantic segmentation[J]. *Proceedings of the IEEE Conference on Computer Vision and Pattern Recognition*, 2015: 3431-3440.
- [17] Agostinelli F, Anderson MR, Lee H. Adaptive multi-column deep neural networks with application to robust image denoising[J]. *Advances in Neural Information Processing Systems*, 2013: 1493-1501.
- [18] Dong C, Loy CC, He K, et al. Image super-resolution using deep convolutional networks[J]. *IEEE Transactions on Pattern Analysis and Machine Intelligence*, 2016, 38(2): 295-307.
- [19] Cha KH, Hadjiiski L, Samala RK, et al. Urinary bladder segmentation in CT urography using deep-learning convolutional neural network and level sets[J]. *Medical Physics*, 2016, 43(4): 1882-1896.
- [20] Shin HC, Orton MR, Collins DJ, et al. Stacked autoencoders for unsupervised feature learning and multiple organ detection in a pilot study using 4d patient data[J]. *IEEE Transactions on Pattern Analysis and Machine Intelligence*, 2013, 35(8): 1930-1943.
- [21] Würfl T, Ghesu FC, Christlein V, et al. *Deep Learning Computed Tomography*[M]. Berlin: Springer International Publishing, 2016.
- [22] Hu C, Yi Z, Zhang W, et al. Low-dose ct via convolutional neural network[J]. *Biomedical Optics Express*, 2017, 8(2): 679-694.
- [23] Zhang H, Li L, Qiao K, et al. Image prediction for limited-angle tomography via deep learning with convolutional neural network[J]. *ArXiv preprint ArXiv: 1607. 08707*, 2016.
- [24] Park HS, Choi JK, Seo JK. Characterization of metal artifacts in X-ray computed tomography[J]. *Communications on Pure and Applied Mathematics*, 2017, 70(11): 2191-2217.
- [25] Park HS, Chung YE, Seo JK. Computed tomographic beam-hardening artefacts: Mathematical characterization and analysis[J]. *Philosophical Transactions*, 2015, 373(2043).
- [26] Jia Y, Shelhamer E, Donahue J, et al. Caffe: Convolutional architecture for fast feature embedding[C]//*ACM International Conference on Multimedia*. 2014: 675-678.

工业 X 射线 CT 中基于深度学习的射束硬化伪影抑制方法

周丽平, 孙怡[✉], 程凯, 余建桥

(大连理工大学信息与通信工程学院, 辽宁 大连 116024)

摘要: 利用工业 CT 进行无损检测时, 由于实际 X 射线源的宽能谱特性, 目前现有的大部分重建算法得到的图像含有射束硬化伪影。射束硬化伪影降低了图像的质量, 影响了 CT 图像应用, 如 CT 图像诊断等。本文提出一种基于深度学习的减少硬化伪影的方法, 用大量含有硬化伪影的断层图像作为输入, 用相应的在固定能量下重建的不含硬化伪影的图像作为输出来训练卷积神经网络。通过建立含有硬化伪影的断层图像与不含硬化伪影的断层图像之间的映射关系, 来抑制硬化伪影。实验结果证明了本文所提方法在降低 CT 图像硬化伪影上的有效性。

关键词: 射束硬化; 计算机断层成像; 深度学习; 卷积神经网络



作者简介: 周丽平 (1990—), 女, 大连理工大学, 信息与通信工程专业硕士研究生, 研究方向为 CT 图像重建及伪影消除, Tel: 15242673149, E-mail: zhoulp@mail.dlut.edu.cn; 孙怡[✉] (1964—), 女, 大连理工大学教授, 主要从事立体成像技术、图像处理与分析、图像技术应用研究, Tel: 0411-84707849, E-mail: lslwf@dlut.edu.cn。